Journal of Thermal Analysis, Vol. 48 (1997) 1249-1262

CRYSTAL STRUCTURES AND MELTING THERMODYNAMICS OF N-ACETYLSARCOSINAMIDE AND N-ACETYL-L-ISOLEUCINAMIDE

R. Puliti[a], *C. De Sena*[a] *and C. Giancola*[b]

[a]Istituto per la Chimica di Molecole di Interesse Biologico*, C. N. R. Via Toiano 6, 80072 Arco Felice-Napoli
[b]Dipartimento di Chimica dell'Università "Federico II" di Napoli, Via Mezzocannone 4, 80134 Napoli, Italy

(Received July 9, 1996)

Abstract

Crystal structures together with enthalpies and temperatures of fusion of two substituted amino acids, N-acetylsarcosinamide (NASarA) and N-acetyl-L-isoleucinamide (NAIA), were determined by single crystal X-ray analysis and differential scanning calorimetry, respectively. The results were compared with those of some analogous amino acid derivatives previously studied. The detailed knowledge of crystallographic parameters is undoubtedly useful for discussing the thermodynamic results and rationalizing the fusion behaviour, owing to the rather poor knowledge of the molecular interactions occurring in the melt.

Keywords: crystal structures, enthalpies and entropies of fusion, peptides

Introduction

Globular proteins are molecules characterized, among other exceptional properties, by very high packing densities unusual for most of organic molecules in the liquid state [1–4]. So for globular proteins, the concept of "crystal molecule", namely a crystal of molecular dimensions, was proposed [5]. From this point of view, the physico-chemical characterization of crystalline solids of small polar molecules, in particular peptide and amino acid derivatives, is of wide interest for understanding the intramolecular forces that stabilize enzymes and proteins.

This paper forms part of a program devoted to the study of crystal structures and thermodynamics of the transitions undergone by peptide and amino acid derivatives [6–8]. The substances considered in this study are the N-acetylsarcosinamide (NASarA) and the N-acetyl-L-isoleucinamide (NAIA).

* Associated to the National Institute for the Chemistry of Biological Systems-CNR

0368–4466/97/ $ 5.00

John Wiley & Sons Limited
Chichester

While thermodynamic properties of NASarA resemble at all those of the parent glycine derivative (NAGA), the NAIA properties attracted the attention because their values, likewise the β-branched valine derivative, are very high in comparison with those observed for other substances of this family. The N'-methyl derivatives also show the same analogies when compared with other N'-methyl peptidoamides [9].

The crystal properties of NASarA, viceversa, remarkably differ from those of NAGA and isomeric NAAA (the alanine derivative), owing to the presence of methyl group that limits the possibility to establish hydrogen bonds: only four shared interactions of this kind are possible, all being effective in the crystal. On the other hand several analogies between the crystal structures of NAIA and L-valine derivative (NAVA) were found. Either molecules show more compact shapes and result more efficaciously packed in the crystal than the N-acetyl-L-leucinamide molecules.

Experimental

Materials

The N-acetylsarcosinamide (NASarA) was a kind gift of Prof. T. H. Lilley and the preparation was previously described [10]. N-acetyl-L-isoleucinamide (NAIA) was the commercial product (Bachem).

Crystal data and structure determinations

N-acetylsarcosinamide

Single crystals of NASarA were obtained as colourless prisms by slow evaporation from an ethanol solution. A sample of size 0.32×0.15×0.06 mm was selected for the crystallographic study. Accurate cell parameters were obtained by least-squares refinement of the setting angles of 25 reflections at medium θ ($26^\circ < \theta < 29^\circ$), using graphite monochromatized CuK_α radiation and an Enraf-Nonius CAD-4F diffractometer on line with a MicroVAX Digital computer. 1379 independent reflections ($\theta_{max}=74^\circ$) were collected at room temperature using ω-2θ scan mode as suggested by peak-shape analysis. During the data collection, the intensities of four standard reflections were monitored every 4 h (fluctuations within 3%) in order to check the crystal and equipment stability. No significant intensity decay was observed. The intensities were corrected for Lorentz and polarization factors, but not for absorption effect ($\mu=7.94\ cm^{-1}$). The structure was solved by direct methods using MULTAN11/82 package [11]. The positional and anisotropic temperature parameters for non-hydrogen atoms were refined by full-matrix (on F) least-squares method. At convergence, all hydrogens were unambiguously located on a difference Fourier map and were refined as isotropic atoms in the last refinement cycles. The final discrepancy index $R=\Sigma\ ||Fo|-|Fc||/\Sigma|Fo|$ was 0.032 for 1265 observed reflections with $I \geq 2.5\sigma(I)$; $Rw=0.038$ with $w^{-1}=\sigma^2=\sigma^2(Fo)+(0.02Fo)^2+0.1$, $S=0.89$, $(\Delta/\sigma)_{max}=0.01$ and 123 refined parameters including the extinction coefficient $=1.03(6)\cdot10^{-5}$ [12]. No residual electron density was outside the range: -0.10–$0.12\ eÅ^{-3}$.

N-acetyl-L-isoleucinamide

The crystallization of this substance was troubled us much because of strong difficulties in obtaining single crystals suitable for a X-ray study. All samples, obtained from various solvents and using many crystallization procedures and different temperature ranges, showed reflections with very wide angular spread, index of accentuated mosaicity in the crystals. The unavoidable choice of the ω scan mode with $\Delta\omega > 3$ degrees produced data collections strongly uncorrected that, even if allowed the rough structure interpretation (SIR92 package) [13], prevented any reliable refinement because of the high number of unobserved reflections. At least, by persevering endurance, samples sufficiently ordered were obtained by a very slow concentration process of an ethyl acetate:ethyl ether solution (4:1 ratio) using carefully controlled temperature gradient. A single crystal of size 0.35×0.05×0.03 mm was employed for a tridimensional data collection using ω–θ scanning. Really, the shape of reflections still suggested the ω-scan mode but this type of scansion was rejected because it causes underestimation of the weak reflections (i.e. increasing background/peak ratio). 2078 independent reflections were collected up to $\theta_{max} = 75°$. The data collection procedure and intensity correction were as before described for NASarA. The anisotropic refinement was carried out by full matrix least-squares method for the non-H atoms of the two molecules forming the asymmetric unit in the crystal. At convergence, all hydrogens were generated at the expected positions and included in the last refinement cycles as fixed atoms with temperature factors set equal to B_{eq} of parent atom. The final discrepancy index R was 0.077 for 1361 observed reflections with $I \geq 2.5\sigma(I)$ and 216 refined parameters. $Rw = 0.086$ with $w^{-1} = \sigma^2(Fo) + (0.02Fo)^2 + 1$; $S = 0.93$; $(\Delta/\sigma)_{max} = 0.01$. Residual electron densities were in the range: –0.32–0.37 eÅ^{-3}.

Crystal data of the two structures are summarized in Table 1. Final atomic parameters for NASarA and NAIA (umprimed and primed labels refer to the two independent molecules, respectively) are given in Table 2.

For the crystallographic work the equipment of the C.I.M.C.F. of the University "Federico II" of Naples was used. All calculations were performed using Enraf-Nonius SDP software [14] on a MicroVAX 3100 computer. Atomic scattering factors were taken from Cromer and Waber [15]. Structure factors, complete molecular geometries and anisotropic thermal parameters for both the structures, together with the hydrogen parameters for NAIA, have been deposited.

Calorimetry

Temperatures and enthalpies of fusion were determined using a Perkin Elmer differential scanning calorimeter DSC-7. The dried samples were gently compressed into aluminium crucibles and weighed using a Mettler microelectrobalance. The runs started from room temperature to check the presence of solid-solid transitions or pre-fusion decompositions. A heating rate of 2 K min^{-1} was used in all the measurements. Enthalpy and temperature calibrations were performed using high purity Indium. Baselines were obtained with empty crucibles at the same conditions

Table 1 Crystal data

	N-acetylsarcosinamide (NASarA)	N-acetyl-L-isoleucinamide (NAIA)
Formula	$C_5H_{10}N_2O_2$	$C_8H_{16}N_2O_2$
Molecular weight	130.15	172.23
Space group	$P2_1/n$	$P2_1$
a/Å	6.151(1)	4.846(2)
b/Å	13.502(2)	30.609(8)
c/Å	8.209(1)	7.050(3)
β/°	96.32(8)	110.09(5)
V/Å^3	677.6(2)	982.1(8)
Z	4	4
D_{calc}/g cm^{-3}	1.276	1.165
Radiation used	CuK_α	CuK_α
θ_{max}/°	74	75
Independent reflections	1379	2078
Observed reflection [$I > 2.5\sigma(I)$]	1263	1361
Refined parameters	123	216
Final discrepancy index: R	0.032	0.077
Weighed R factor $w^{-1}=[\sigma^2Fo+(0.02Fo)^2+1]$	0.038	0.086

as the measurements. For baseline subtractions and peak area integrations a manufacturer computer program was used.

The fusion temperatures T_f were directly obtained from the onset temperatures, i.e. the incipient transition temperatures. The molar enthalpies $\Delta_f=H_m$ were determined by peak area of the calorimetric profiles. The molar entropies were instead calculated quantities: $\Delta_f=S_m=\Delta_fH_m/T_m$. Each reported thermodynamic value was the average of at least five experiments.

Results and discussion

Crystal structures

Views of NASarA and NAIA molecules showing the conformations adopted in the respective crystals are reported in Fig. 1. Intramolecular geometries are given in Table 3 for NASarA and in Table 4 for NAIA structures.

In the NASarA molecule, bond lengths and bond angles are in good agreement with the corresponding values observed in similar structures [7, 8] and they do not show significant differences from the expected values for small peptide crystals [16, 17]. The molecular conformation falls within F region of the conventional φ–ψ map

Table 2 Fractional coordinates and equivalent isotropic thermal parameters ($Å^2$) with e.s.d.'s in parentheses

$$B_{eq} = 1/3\sum_i \sum_j b_{ij} \cdot a_i^* a_i \cdot a_j^* a_j$$

	x	y	z	B_{eq}		x	y	z	B_{eq}
				N-acetylsarcosinamide (NASarA)					
O1	0.5068(2)	0.24258(7)	0.8179(1)	4.74(2)	H1	0.193(3)	0.206(1)	0.499(2)	3.7(3)
O2	0.3603(1)	0.50626(6)	0.7529(1)	4.68(2)	H2	0.238(2)	0.134(1)	0.653(2)	3.0(3)
N1	0.6217(1)	0.41173(7)	0.6636(1)	3.64(2)	H3	0.316(2)	0.386(1)	0.558(2)	3.5(3)
N2	0.2720(2)	0.19252(7)	0.6059(1)	4.00(2)	H4	0.508(2)	0.325(1)	0.470(2)	3.3(3)
C1	0.4583(2)	0.34716(8)	0.5794(1)	3.64(2)	H5	0.873(3)	0.362(2)	0.552(2)	7.0(5)
C2	0.4139(2)	0.25631(8)	0.6798(1)	3.22(2)	H6	0.895(3)	0.326(2)	0.740(2)	6.3(5)
C3	0.5566(2)	0.48762(8)	0.7507(1)	3.45(2)	H7	0.943(3)	0.440(2)	0.674(2)	7.0(5)
C4	0.8506(2)	0.38452(9)	0.6561(2)	5.74(3)	H8	0.808(3)	0.509(1)	0.936(2)	6.2(5)
C5	0.7273(2)	0.55023(9)	0.8460(2)	4.94(3)	H9	0.661(3)	0.608(1)	0.892(2)	5.5(4)
					H10	0.844(3)	0.573(1)	0.776(2)	5.1(4)

Table 2 Continued

	x	y	z	B_{eq}		x	y	z	B_{eq}
				N-acetyl-L-isoleucinamide (NAIA)					
O1	–0.235(1)	0.0000*	0.2818(8)	4.5(2)	O1′	0.229(1)	0.2000(3)	–0.2633(8)	4.4(2)
O2	0.725(1)	0.0368(2)	0.7594(8)	4.0(1)	O2′	–0.257(1)	0.1668(2)	0.2154(8)	3.8(1)
N1	0.236(1)	0.0224(2)	0.6464(9)	2.7(1)	N1′	0.114(1)	0.1783(3)	0.0965(9)	2.9(1)
N2	0.139(1)	0.0022(3)	0.1542(9)	3.6(2)	N2′	–0.260(1)	0.1967(3)	–0.384(1)	4.0(2)
C1	0.251(2)	–0.0134(3)	0.513(1)	2.7(2)	C1′	–0.017(2)	0.2144(3)	–0.029(1)	2.9(2)
C2	0.039(2)	–0.0039(3)	0.308(1)	3.3(2)	C2′	–0.009(2)	0.2038(3)	–0.236(1)	3.2(2)
C3	0.470(2)	0.0460(3)	0.760(1)	3.0(2)	C3′	–0.001(2)	0.1561(3)	0.215(1)	2.5(2)
C4	0.421(2)	0.0815(4)	0.887(1)	4.1(2)	C4′	0.167(2)	0.1196(3)	0.343(1)	3.6(2)
C5	0.187(2)	-0.0569(3)	0.589(1)	3.4(2)	C5′	0.129(2)	0.2576(3)	0.048(1)	3.3(2)
C6	0.415(2)	–0.0666(4)	0.803(1)	4.3(2)	C6′	0.108(2)	0.2684(4)	0.256(1)	4.1(2)
C7	0.327(2)	–0.1046(4)	0.909(1)	5.3(3)	C7′	0.306(2)	0.3047(4)	0.360(2)	5.2(3)
C8	0.179(2)	–0.0939(4)	0.442(1)	4.9(3)	C8′	0.009(2)	0.2939(4)	–0.098(2)	6.0(3)

*Fixed to define the origin

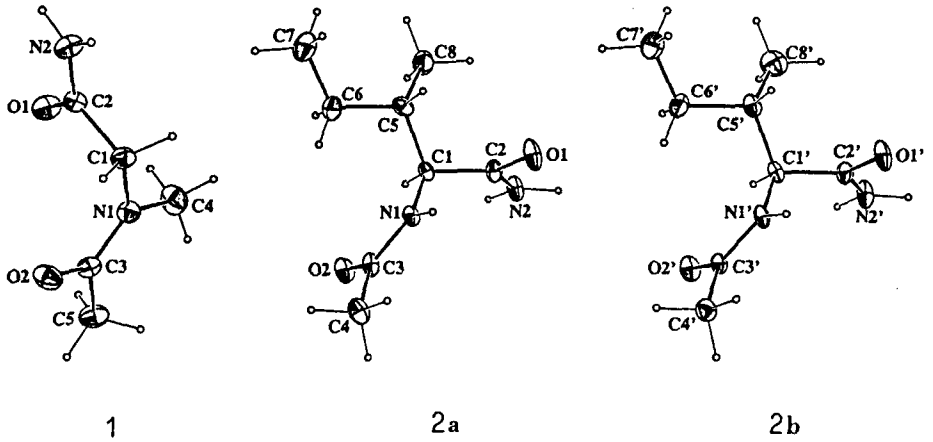

Fig. 1 Perspective views of the molecules with the atomic labelling schemes for non-H atoms: **1** NASarA, **2a** and **2b** the two independent molecules of the NAIA crystal. Thermal ellipsoids are at 30% probability error

for peptides [18]. A perspective view of the crystal packing is reported in Fig. 2. The amide group is the only potential H-bond donor since the methyl substituent at N1 makes it unable to form hydrogen bonds. The NH_2 group is involved in two hydrogen interactions with the carbonyl oxygens O1 and O2 of two molecules related by symmetry centre. In this way each NASarA molecule shares four H-bonds with four molecules. The H-bond geometry and symmetries of the acceptor atoms are given in Table 5. In the crystal, hydrogen bonds interconnect molecules referred by

Table 3 Molecular geometry for N-acetylsarcosinamide (NASarA) with e.s.d.'s in parentheses

Bond lengths/Å					
O1–C2	1.227(1)	N1–C3	1.336(1)	C1–C2	1.519(2)
O2–C3	1.236(1)	N1–C4	1.463(2)	C3–C5	1.499(2)
N1–C1	1.447(1)	N2–C2	1.325(1)		
Bond angles/°					
C1–N1–C3	118.97(9)	O1–C2–N2	122.8(1)	O2–C3–N1	121.0(1)
C1–N1–C4	116.7(1)	O1–C2–C1	122.02(9)	O2–C3–C5	120.4(1)
C3–N1–C4	124.2(1)	N2–C2–C1	115.20(9)	N1–C3–C5	118.6(1)
N1–C1–C2	112.61(9)				
Selected torsion angles/°					
C3–N1–C1–C2	φ	–94.3(1)	C4–N1–C3–C5		0.7(2)
C4–N1–C1–C2		81.5(1)	N1–C1–C2–N2	ψ	–177.4(1)
C1–N1–C3–C5	ω′	176.2(1)			

Table 4 Molecular geometry for N-acetyl-L-isoleucinamide (NAIA) with e.s.d.'s in parentheses

Bond	O1–C2	1.28(1)	C1–C5	1.51(1)	O1′–C2′	1.24(1)	C1′–C5′	1.51(1)
lengths/Å	O2–C3	1.27(1)	C3–C4	1.48(1)	O2′–C3′	1.28(1)	C3′–C4′	1.49(1)
	N1–C1	1.46(1)	C5–C6	1.56(1)	N1′–C1′	1.42(1)	C5′–C6′	1.54(1)
	N1–C3	1.350(9)	C5–C8	1.52(1)	N1′–C3′	1.34(1)	C5′–C8′	1.49(2)
	N2–C2	1.34(1)	C6–C7	1.52(2)	N2′–C2′	1.323(8)	C6′–C7′	1.49(1)
	C1–C2	1.49(1)			C1′–C2′	1.50(1)		
Bond	C1–N1–C3	124.5(7)	O2–C3–N1	119.8(8)	C1′–N1′–C3′	126.3(7)	O2′–C3′–N1′	118.7(7)
angles/°	N1–C1–C2	108.0(7)	O2–C3–C4	121.6(7)	N1′–C′1–C2′	106.4(7)	O2′–C3′–C4′	121.2(8)
	N1–C1–C5	111.9(7)	N1–C3–C4	118.6(7)	N1′–C1′–C5′	113.8(6)	N1′–C3′–C4′	120.1(7)
	C2–C1–C5	111.0(7)	C1–C5–C6	110.4(7)	C2′–C1′–C5′	111.8(8)	C1′–C5′–C6′	110.6(8)
	O1–C2–N2	121.0(6)	C1–C5–C8	112.3(8)	O1′–C2′–N2′	120.8(8)	C1′–C5′–C8′	112.3(7)
	O1–C2–C1	119.6(8)	C6–C5–C8	111.0(8)	O1′–C2′–C1′	120.4(6)	C6′–C5′–C8′	111.1(9)
	N2–C2–C1	119.3(7)	C5–C6–C7	113.4(8)	N2′–C2′–C1′	118.7(8)	C5′–C6′–C7′	112.7(9)
Selected	C3–N1–C1–C2	φ	–125.9(8)		C3′–N′1–C1′–C2′	φ	–128.7(8)	
torsion	C3–N1–C1–C5		111.7(8)		C3′–N1′–C1′–C5′		107.6(9)	
angles/°	C1–N1–C3–C4	ω′	179.5(7)		C1′–N1′–C3′–C4′	ω′	–178.3(7)	
	N1–C1–C2–N2	ψ	116.9(9)		N1′–C1′–C2′–N2′	ψ	112.4(9)	
	C5–C1–C2–N2		–120.0(9)		C5′–C1′–C2′–N2′		–122.7(9)	
	N1–C1–C5–C6	$\chi^{1,1}$	–60.1(9)		N1′–C1′–C5′–C6′	$\chi^{1,1}$	–61.5(9)	
	N1–C1–C5–C8	$\chi^{1,2}$	175.4(7)		N1′–C1′–C5′–C8′	$\chi^{1,2}$	173.7(8)	
	C2–C1–C5–C6		179.2(7)		C2′–C1′–C5′–C6′		177.8(7)	
	C1–C5–C6–C7	χ^{2}	167.1(8)		C1′–C5′–C6′–C7′	χ^{2}	166.5(8)	

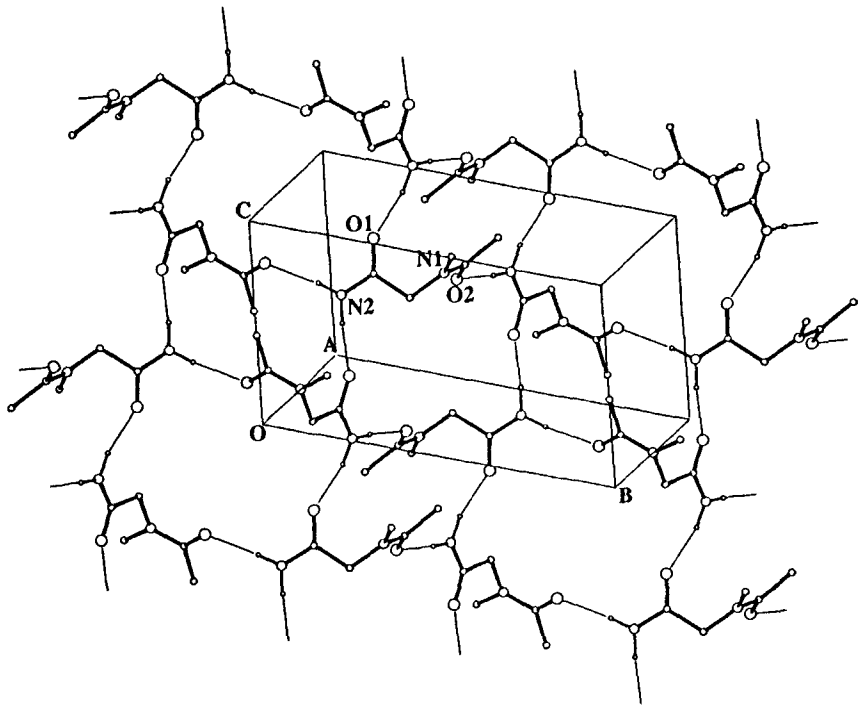

Fig. 2 Perspective view of the crystal packing of NASarA. For clarity, only O and N atoms are labelled. Thin lines indicate hydrogen bonds, the symmetry of acceptors is reported in Table 5

glide symmetry and form polar layers approximately parallel to the **b,a+c** plane. The shortest van der Waals interaction is Cl.....$C3_{(1-x,1-y,1-z)}$= 3.503(2)Å.

As reported in the experimental section, the quality of NAIA crystals did not permit a fine refinement of the structure and the geometrical parameters cannot be used confidently because of large errors associated. However that does not invalidate the conformational data and intermolecular interactions at all and even less the thermodynamic considerations after discussed. The independent part of the unit cell contains two molecules (*A*, umprimed labels and *B*, primed labels) that have very similar geometrical and conformational parameters. The pairs of φ, ψ torsion angles (Table 4) let the peptidic backbones within *E* region of the conventional Zimmerman map [18]. The side chains of the Ile residues present in both the molecules (g^-,*t*)*t* conformations, where the two letters in parentheses indicate the orientations of the two C^γ atoms with respect to N1 [19]. The conformations (g^-,*t*) type are the most frequently observed in β-branched residues of small-peptide structures. In fact, the observed distributions are 44% for (g^-,*t*) conformers, against 28 and 27% for (*t*, g^+) and (g^+,g^-) types, respectively because, in both the more rare conformers, one methyl group is always in the least favourable *gauche*$^+$ position.

The crystal packing is ruled by intermolecular hydrogen bonds which link molecules only of the same type and form layers of molecules translated along the *ac*

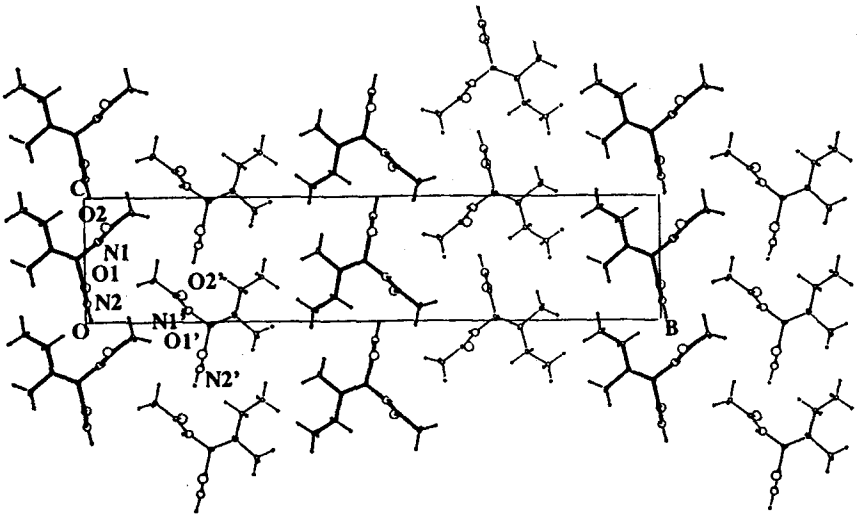

Fig. 3 Crystal packing of NAIA projected along the *a* direction. Thick and thin lines indicate the *A* and *B* independent molecules, respectively. Only O and N atoms are labelled

plane. The patterns of H-bonds, see Table 5, are strictly analogous for the two independent NAIA molecules. Figure 3 shows the molecular arrangement along the *a* direction. Layers formed by *A* molecules (thick lines) alternate, along the *b* direction, with layers of *B* molecules (thin lines). In each layer, rows of molecules translated along the *a* direction are linked by two H-bonds involving peptide nitrogens

Table 5 Hydrogen-bonding geometry (Å, °) with e.s.d. values in parentheses

D–H·····A	D·····A	H·····A	D–H·····A	Symmetry code of acceptor
		N-acetylsarcosinamide (NASarA)		
N2–H1·····O1	2.858(1)	1.91(1)	165.(1)	(i)
N2–H2·····O2	2.922(1)	2.01(1)	175.(1)	(ii)
Symmetry of acceptor:	(i) $x-1/2$, $1/2-y$, $z-1/2$; (ii) $1/2-x$, $y-1/2$, $3/2-z$			
		N-acetyl-L-isoleucinamide (NAIA)		
N1–H1·····O2	2.883(9)	1.95	160.	(i)
N2–H2·····O1	2.850(8)	1.90	166.	(ii)
N2–H3·····O2	3.009(8)	2.05	170.	(iii)
N'1–H1·····O'2	2.893(8)	2.00	152.	(ii)
N'2–H2·····O'1	2.883(9)	1.93	169.	(i)
N'2–H3·····O'2	2.972(9)	2.00	176.	(iv)
Symmetry of acceptor:	(i) $x-1$, y, z; (ii) $x+1$, y, z; (iii) $x-1$, y, $z-1$; (iv) x, y, $z-1$			

N1 with acetyl oxygens O2 and amidic N2 with O1 atoms, respectively. The third H-bond connects adjacent rows along the *c* direction through amide groups and O2 acetyl oxygens which act as double acceptors. The H-bonds layers separate, along the **b** axis, two apolar regions containing alternately the acetyl groups and Ile side chains of both the *A* and *B* molecules.

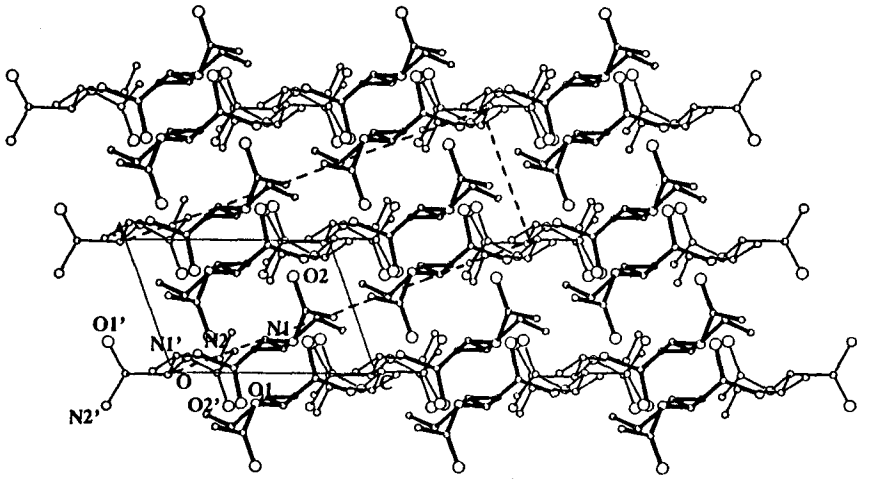

Fig. 4 Crystal packing of NAIA projected onto the *a, c* plane. Thick and thin lines indicate the *A* and *B* independent molecules, respectively. Dashed lines show the centered *pseudo* orthorhombic cell

In the NAIA crystal, layers of *A* and *B* molecules are related each other by a *pseudo* two fold axis perpendicular to *ab* plane, as so as the molecular arrangement falls in a *pseudo* orthorhombic centered space group ($B22_12$) that is indicated by dashed lines in Fig. 4. The presence in this structure of layers of molecules strongly linked by H-bonds which alternate, along the **b** axis, with regions of weak van der Waals interactions, suggests a possible explanation of the difficulties met in the obtaining of well ordered crystal samples. In fact, the adjacent molecular layers can arrange in different ways in the crystal, without trouble significantly the short-range intermolecular interactions. That, however, destroys the exact crystallographic symmetry along the *b* direction and favours the making of lamellar structures and high mosaicity in the crystals.

Thermodynamics of fusion

Thermodynamic parameters for NASarA and NAIA are reported in Table 6 together with the corresponding values of some N-acetylamides previously determined [6, 20]. The substances reported in the Table 6 can be split into two groups formed by the first three and the last three compounds, respectively. In the first group, it can be observed that the data of NASarA resemble more those of glycine derivative (NAGA) than those of isomeric L-alanine derivative (NAAA). Really, in the crystals of NASarA each molecule is linked to neighbour molecules by only two

Table 6 Thermodynamic parameters pertaining to the fusion of N-acetylamides of some amino acids

	T_f/ K	$\Delta_f H_m$/ kJ mol^{-1}	$\Delta_f S_m$/ J mol^{-1} K^{-1}	H-bonds/ (per molecule)	D_{cryst}/ g cm^{-3}
N-Ac-Gly-NH_2[a,b] (NAGA)	410.9(1)	27.0(1)	65.7(3)	3	1.319
N-Ac-Sar-NH_2 (NASarA)	412.7(1)	27.4(3)	66.4(7)	2	1.276
N-Ac-L-Ala-NH_2[a,b] (NAAA)	435.4(1)	23.7(3)	54.4(7)	3	1.203
N-Ac-L-Val-NH_2[a,c] (NAVA)	509.0(2)	36.9(4)	72.5(8)	3	1.135
N-Ac-L-Ile-NH_2[a] (NAIA)	529.6(2)	41.8(1)	78.9(2)	3	1.165
N-Ac-L-Leu-NH_2[a,b] (NALA)	401.4(3)*	17.4(3)	43.3(8)	2	1.125

[a] From [6], [b] From [21], [c] From [20]

*Another broad peak is present with a maximum at 382 K and $\Delta_{trans}H$=0.3(1) kJ mol^{-1}

hydrogen bonds and the crystal density is a little lower than that of NAGA (i.e. the intermolecular interactions are less effective). In the crystals of NAAA, as well as of NAGA, each molecule is instead linked by three hydrogen bonds to the neighbours. In spite of that, the $\Delta_f H_m$ and $\Delta_f S_m$ values of the sarcosine derivative result higher than that of NAAA. The $\Delta_f S_m$ values of NASarA are similar to that of NAGA, so indicating a comparable gain of freedom for each molecule in the two melts. However the enthalpies of fusion require a more complex rationale. In fact, the $\Delta_f H_m$ value for NASarA can be explained assuming that in liquid phase the intermolecular interactions are in large part weak and unstable, while in the case of NAGA the residual and short-living interactions (H-bonds, dipolar interactions, dispersive forces) are still partially operative, so the differences between the crystal and liquid states only fortuitously make comparable thermodynamic parameters for the two substances. The higher value of T_f for L-alanine derivative, *viceversa*, comes from the ratio of the relatively low values of both $\Delta_f H_m$ and $\Delta_f S_m$, and does not represent an independent absolute indication of the crystal structure stability.

Within the second group of substances, the thermodynamic properties pertaining the fusion process of NAIA are much more near to those of the L-valine derivative (NAVA) than to those of the isomer N-acetyl-L-leucinamide. The higher values of T_f for NAIA and NAVA, when compared to those of NALA, are imputable to the $\Delta_f H_m$ values more than $\Delta_f S_m$, as it is possible to deduce from Table 6. The number of hydrogen bonds (three instead of two) and the little higher packing densities make more effective in the solid state the intermolecular interactions of NAIA and NAVA than those of NALA. Therefore, during the fusion of the former two sub-

stances it needs to break more intermolecular interactions than for NALA. Moreover, an additional energy contribution is required for the activation of several hindered rotational states, around the C^{α}-C^{β} bond, which are absent for the γ-branched enantiomer (NALA). On the other hand the major gain of entropy attained during the fusion by NAIA and NAVA is due to their compact shapes which allow large rotational freedom of the overall molecule. It is likely that in the melt the more flexible γ-branched side chain of NALA promotes intermolecular contacts that interfer with the free rotation.

Finally, it must be noted that NAIA and NAVA show $\Delta_f H_m$ and $\Delta_f S_m$ values higher than those measured for NAGA and NAAA whose crystals are characterized by equal number of hydrogen bonds per molecule but higher packing densities. Really, several effects can contribute to these differences: for the higher homologues it need to break, per each molecule, a major number of intermolecular interactions which are probably also a little stronger owing to the apolar local environment. The activation of the hindered internal rotations of the side chains also gives its contribution. All the corresponding degrees of freedom involved work to make entropy changes higher for NAIA and NAVA.

Conclusions

The crystal stability of polar organic molecules cannot always be estimated by the T_f values only, they resulting from a combination of enthalpic and entropic effects. Moreover, the detailed knowledge of the thermodynamic quantities characterizing the fusion process are not always sufficient to provide the complete information about the crystal structure stability, owing to the ignorance of the complex molecular interactions in the liquid state. The comparison between the fusion thermodynamic parameters and the crystallographic data, that allow us to get a very deep insight in the solid state, appears instead to be a powerful tool for studying these systems.

* * *

The authors thank prof. Guido Barone for useful discussions.

References

1 J. Bello, J. Theor. Biol., 68 (1977) 139.
2 F. M. Richards, J. Mol. Biol., 82 (1974) 1.
3 C. Chothia, Nature, 248 (1974) 338.
4 C. Chothia and J. Janin, Nature, 256 (1975) 705.
5 A. M. Liquori, Quaterly Rev. Biophys., 2 (1969) 65.
6 G. Barone, C. Giancola, T. H. Lilley, C. A. Mattia and R. Puliti, J. Thermal Anal., 38 (1992) 2771.
7 R. Puliti, C. De Sena and C. A. Mattia, Acta Cryst., C52 (1996) 1820 and references cited therein.
8 R. Puliti, G. Barone, C. Giancola and C. A. Mattia, J. Mol. Struc., 382 (1996) 197.
9 L. Abate and G. Della Gatta, private communication.

10 T. H. Lilley, in M. N. Jones (Ed.), Biochemical Thermodynamics, Elsevier, Amsterdam 1988, p. 1-52.
11 P. Main, S. J. Fiske, S. E. Hull, L. Lissinger, G. Germain, J.-P. Declercq and M.M. Woolfson, MULTAN11/82. A System of Computer Programs for the Automatic Solution of Crystal Structures from X-ray Diffraction Data. University of York, UK and Louvain, Belgium, 1982.
12 G. H. Stout and L. H. Jensen, In X-Ray Structure Determination. Macmillan, New York 1968, p. 409-412.
13 A. Altomare, G. Cascarano, C.Giacovazzo and A. Guagliardi, J. Appl. Cryst., 26 (1993) 343.
14 B. A. Frenz and Associates, SDP Structure Determination Package,College Station, TX, USA and Enraf Nonius, Delft, The Netherlands, 1985.
15 D. T. Cromer and J. T. Waber, in International Tables for X-ray Crystallography, Vol. IV, Kynoch Press, Birmingham, Kluwer Academic Publishers, Dordrecht 1974.
16 T. Ashida, Y. Tsunogae, I. Tanaka and T. Yamane, Acta Cryst., B43 (1987) 212.
17 R. A. Engh and R. Huber, Acta Cryst., A47 (1991) 392.
18 S. S. Zimmerman, M. S. Pottle, G. Némethy and H. A. Scheraga, Macromolecules, 10 (1977) 1.
19 E. Benedetti, G. Morelli, G. Némethy and H. A. Scheraga, Int. J. Peptide Protein Res., 22 (1983) 1.
20 R. Puliti, C.A. Mattia, G. Barone, G. Della Gatta and D. Ferro, Thermochim. Acta, 162 (1990) 229.
21 R. Puliti, C. A. Mattia, G. Barone and C. Giancola, Acta Cryst., C45 (1889) 1554.